Original Article

Photovoltaic Power Plant Performance Improvement with Electric Vehicle Integration: Integrated Control Strategies

Basaralu Nagasiddalingaiah Harish[1], Usha Surendra[2]

1,2Electrical and Electronics Engineering, School of Engineering and Technology, Christ (Deemed to be University), Karnataka, India.

1Corresponding Author : bn.harish@res.christuniversity.in

Abstract - *The combination of Photovoltaic (PV) systems and Electric Vehicles (EVs) holds enormous promise in an era characterized by growing environmental consciousness and sustainable energy solutions. PV technology is a clean, sustainable energy source that produces electricity by utilizing solar energy. Concurrently, EVs' electrification of transportation is a critical step in the direction of lower greenhouse gas emissions and more energy efficiency. Through the use of advanced control systems, this research aims to push the boundaries of current practice in the area of PV and EV integration. Specifically, it focuses on the Icosφ controller and dq controller to regulate voltage, minimize Total Harmonic Distortion (THD), and facilitate bi-directional power flow. A thorough Simulink model is created, simulating a complicated PV-EV-grid system, in order to evaluate the effectiveness of different control mechanisms. This model accommodates the unique characteristics of Plug-in Hybrid Electric Vehicles (PHEVs) and enables a detailed assessment of the percentages of voltage and current THD under different operating situations. It can handle both linear and non-linear loads. Most importantly, the study's findings show that the THD values meet the strict requirements outlined in IEEE519, highlighting the efficiency of the integrated control approaches. The research not only contributes to the advancement of PV and EV technologies but also paves the way for grid-compatible, high-quality power distribution. This endeavor facilitates sustainable energy integration while simultaneously reducing the environmental footprint, making substantial strides toward a greener and more energy-efficient future.*

Keywords - Photovoltaic (PV), Electric Vehicles (EVs), Control strategies, Total Harmonic Distortion (THD), Icos φ controller.

1. Introduction

In light of the ongoing global decarbonisation efforts, there has been a remarkable surge in the adoption of distributed photovoltaic (PVs) and Electric Vehicles (EVs) within the power grid. Recent data from the International Energy Agency underscores the exponential growth in EV numbers over the past decade, with the global EV stock reaching new heights, with light-duty passenger vehicles constituting the majority of these applications [1].

In 2022, the solar Photovoltaic (PV) market continued its impressive growth, achieving a remarkable milestone by adding around 191 GW of new capacity (source: IRENA, 2023). This extraordinary surge in capacity marked the most substantial annual increase ever documented and propelled the total global solar PV capacity to an impressive 1,133 GW [2].

While the rapid integration of EVs and PVs into the grid is a positive step toward decarbonizing power generation and transportation, it presents unique challenges. Voltage violations and fluctuations occur from the inherent uncertainties in PV power generation and the stochastic charging behaviors of EVs, which make maintaining voltage quality more difficult.

Distribution network voltage control has traditionally been achieved through the use of switchable Capacitor Banks (CBs) and On-Load Tap-Changing (OLTC) transformers. However, the discontinuous voltage management and sluggish response times of these conventional approaches make them unsuitable for handling fluctuations and voltage deviations in distribution networks with substantial penetrations of electric vehicles and photovoltaics.

In stark contrast, the integration of PVs and EVs into distribution networks involves their connection via fully controllable power electronic converters. This technological advancement empowers them to serve as flexible and responsive voltage support resources, offering innovative solutions to the challenges posed by a grid with a growing presence of EVs and PVs.

Various studies in the literature have explored the integration of PV arrays with E-mobility systems. This

integration, when connected to the grid, helps mitigate the intermittent nature of solar PV arrays while also providing an alternative source for charging [3].

Additionally, Electric Vehicle (EV) batteries have emerged as a valuable energy source, especially considering that EVs spend approximately 90% of their lifetime parked. As a result, the concept of Vehicle-to-Grid (V2G) mode has received detailed attention [4]. Furthermore, researchers have delved into the idea of utilizing surplus solar and battery power by feeding it back into the grid for additional support [5].

Reactive power support, a critical aspect of power system stability, can be efficiently provided by Voltage Source Converters (VSC) with the right control techniques as an alternative to expensive capacitor banks for reactive power compensation. By transferring reactive power from the source to the load, this method also aids in lowering transmission line losses [6].

It is critical to handle the presence of nonlinear loads that pull non-sinusoidal currents from the grid in the context of modern power systems. These nonlinear loads have caused harmonics to be injected into the utility grid; potential remedies have been examined from the charger's point of view when operating in the V2G mode. The goal of these solutions is to improve the grid's overall power quality [7].

Three main levels are used to charge Electric Vehicles (EVs): AC Level 1, AC Level 2, and DC Level 3, which is intended for rapid charging. There have been many notable contributions to the field of electrical charging station research, which has been extensively studied [8].

In one study [9], scientists integrated solar PV and wind energy with an AC charging station that included a second-life Li-Ion battery. Because this station was connected to the grid, electricity could move in both directions-importing and exporting. Subsequent research investigated novel control schemes for grid-connected solar power plant quick charging stations. Researchers looked into methods for improving multi-port charging stations [10]. Additionally, a study detailed in [8] presented a charging strategy that divided the charging duration into intervals, strategically minimizing peak energy consumption by the EV fleet during daytime hours, thereby reducing energy costs.

Conventional two-level DC-DC converters have been widely discussed in the context of charging infrastructure. These converters, known for their simplicity and high efficiency, often employ basic topologies like buck and boost converters [9]. Conventional converters, however, have limits when handling medium and high voltage levels, which are typical in fast-charging stations. Their switching components are subjected to higher voltage stress, necessitating the

adoption of more expensive and potent components. This raises the volume and complexity of the system in addition to raising the cost.

The use of Multi-Level (ML) converters has become more popular as a strong substitute to address these issues. Reduced output voltage distortion, lower switching losses, and less strain on the devices are only a few benefits of using ML converters [11-14].

These characteristics provide economical and efficient operation, making them a potential alternative for medium and high-voltage applications in the charging infrastructure. Harmonics and reactive power demands are two common Power Quality (PQ) problems in single-phase and three-phase electrical systems. Many setups and tactics have been used to address these issues [15].

Three times the phase current, or neutral line current, is a typical problem in Three-Phase, Four-Wire (3P4W) systems. To address these issues, a number of solutions have been developed, such as three H-bridge variants, normal inverters with an extra fourth leg layout, and the usage of split capacitors in 3P4W arrangements. Neutral current in the 3P4W system is a major issue that can be resolved in a number of ways, including the use of capacitor-split arrangements, four-leg inverters, and three-leg bridge designs. Each approach offers its advantages and disadvantages. For instance, the split capacitor approach requires an additional control loop to balance the voltages and ensure the capacitors at the DC link remain identical [16].

In contrast, the four-leg design entails expanding the standard inverter configuration by one leg in order to accommodate the neutral line current. When compared to the split-capacitor architecture, this topology frequently yields better results [17, 18]. In essence, a bridge circuit with three inverter legs coupled to a capacitor is used. Allowing each phase to be adjusted independently while interacting with the others improves the 3P4W system's controllability.

Accelerated identification of voltage and current disturbances in the power system is essential for resolving PQ issues in real-time cases. Shunt Active Power Filters (APFs) are mostly dependent on how well the reference current is generated in order for them to offset these problems adequately. For effective PQ improvement, accurate reference current generation is essential.

Active Power Filters (APFs) employ a variety of control strategies, each with its own set of characteristics and considerations. Among these strategies, Proportional-Integral Derivative (PID) control techniques [19] are widely utilized, yet they demand the measurement of numerous variables, introducing complexity and resource requirements into the system. Conversely, hysteresis control, noted in [20], is

relatively simpler to implement but typically operates with a high hysteresis band value, which can propagate low-order harmonic distortion and result in increased switching losses, potentially affecting overall system performance.

On the other hand, there are clear benefits to Model-based Predictive Control (MPC), as shown in [21-23]. It has the capacity to control multivariable systems with nonlinearities and limitations and offers a quick dynamic reaction. However, as stated in [24], MPC depends on an accurate system model and uses variable switching frequencies, which can introduce low-order harmonics into the output current and potentially affect the system context of APFs based on seven-level cascade H-bridge converters using particular switching states corresponding to constant reference voltages. Nevertheless, as described in [25-28], these systems include floating capacitors in the DC-link.

Voltage ripples may result from the way these capacitors are charged and discharged based on the direction of the filter current. These ripples have the potential to cause error propagation between the reference values and measured DC-link voltages, which would impair the control system's accuracy and capacity to effectively correct problems with power quality. Through the use of multicarrier Space Vector Pulse Width Modulation (SVPWM) in a three-level inverter system, this research presents a novel way to reduce power quality difficulties.

Enhancing the distribution system's ability to sustain the strict 440V/50Hz requirements at the Point of Common Coupling (PCC) is the major goal, especially when paired with a Photovoltaic (PV) power generation. The main goal of the research is to reduce the power quality disturbances caused by the growing integration of Electric Vehicles (EVs) into the distribution network.

To this end, extensive MATLAB simulations are used. A key component of the research's methodology is the combination of grid-connected PV distributed generation with Plug-in Hybrid Electric Vehicles (PHEVs). The simulation findings indicate that this integrated system has an enhanced power quality profile with respect to Total Harmonic Distortion (THD) and power factor.

Notably, when compared to the I-cosØ operation, the implementation of a DQ-controlled multicarrier SVPWM method shows improved results in terms of THD and power factor. This design's ability to operate in both directions is one of its most amazing qualities, and it makes it ideal for use in smart buildings and sophisticated energy management systems. This research helps to produce more durable and dependable energy systems by addressing power quality issues and proving the efficacy of the suggested inverter and control technique, particularly in light of the growing

penetration of EVs in contemporary distribution networks. The main contributions of this research can be summarized as follows:

- The research introduces and implements advanced control strategies, including the Icos_ controller and dq controller, to regulate voltage and minimize Total Harmonic Distortion (THD) in the context of PV and EV integration.
- The study presents a three-level inverter system with multicarrier Space Vector Pulse Width Modulation (SVPWM), offering a robust and efficient solution for maintaining stringent power quality standards.
- By addressing power quality disturbances associated with the growing integration of Electric Vehicles (EVs) into distribution networks, this research significantly enhances power quality, thus contributing to a more stable and reliable energy infrastructure.
- To assess voltage and current THD percentages under a range of operating settings, including those involving both linear and non-linear loads and Plug-in Hybrid Electric Vehicles (PHEVs), a comprehensive Simulink model has been constructed.

The bidirectional operation of the system makes it highly suitable for applications in smart buildings and advanced energy management systems, contributing to a greener and more energy-efficient future. The paper is structured into several sections. In Section 2, the arrangement of photovoltaic panels, electric vehicle charging infrastructure, grid connection, and the key elements contributing to the system's functionality. Section 3 details the proposed control strategies involving Icos Ø and dq controllers, while Section 4 presents simulation results and discussions regarding voltage and current THD percentages. Section 5 serves as the conclusion, highlighting research contributions and applications.

2. System Configuration

The suggested system configuration, which is shown in Figure 1 and Table 1, is a multi-component structure made to generate, distribute, and manage power effectively while preserving high-quality electrical power. It incorporates a number of components to guarantee the smooth integration of grid connectivity, renewable energy sources, and power supply to various loads.

Let's delve into the system's configuration and structure in more detail: At the heart of the system is the Photovoltaic (PV) array. This array comprises six series-connected panels and 48 parallel-connected panels, collectively harnessing solar energy. It generates electricity when exposed to sunlight. For the PV array to extract as much power as possible, vital factors like voltage at maximum power point (Vmpp) and current at maximum power point (Impp) are crucial.
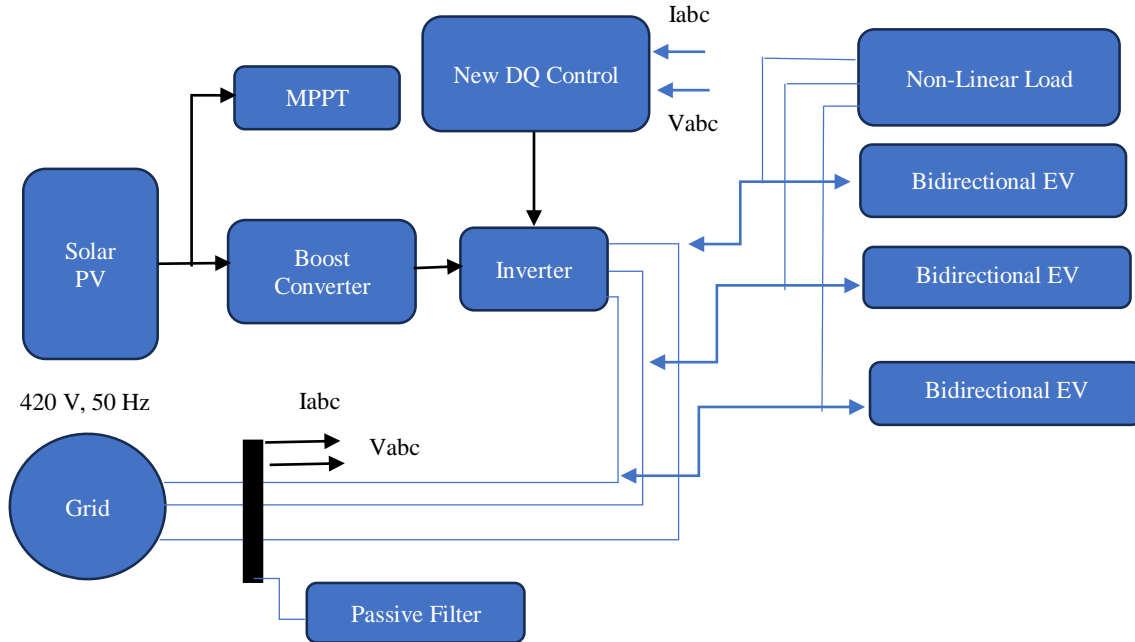
Fig. 1 System configuration

A boost converter is used to modify the voltage of the DC electricity produced by photovoltaic cells. The voltage is changed by this part to make it equal to the necessary Direct Current (DC) link voltage. In order to successfully integrate the power produced by the PV array into the larger system, this phase is essential. After the boost converter, a three-level inverter that uses Sine Vector Pulse Width Modulation (SVPWM) transforms the DC power into Alternating Current (AC) power.

This inverter technology ensures that the AC power generated is of high quality and can be seamlessly synchronized with the grid. SVPWM is a sophisticated control technique that optimizes the generation of clean and efficient AC power. The system is connected to the grid, which serves as a supplementary power source. In cases where the PV array does not generate sufficient electricity, the grid provides the required power.

Additionally, excess power generated by the PV array can be supplied back to the grid. A transformer with a 1:1 voltage ratio is integrated into the system. This transformer is responsible for matching the voltage levels between the grid and the system. It ensures that the power from the grid aligns with the system's voltage requirements, facilitating smooth power exchange.

The system caters to a diverse range of loads, including linear, non-linear, and Electric Vehicle (EV) loads. These loads vary in their power consumption characteristics: An 80 kW linear load represents a constant power consumer that draws a consistent 80 kW of power. The non-linear load, consisting of a rectifier with specified inductance (L) and resistance (R), introduces non-sinusoidal components into the system due to its rectification process. The actual power consumption of this load is not provided, but it is essential to consider its impact on power quality due to harmonic generation.

The system accommodates plug-in electric vehicles for charging. A 120 V li-ion battery with 50 Ah is part of the EV load. The combination of these loads presents potential power quality challenges, particularly due to the introduction of harmonics from non-linear loads and the dynamic nature of EV charging. To address these issues, the system relies on advanced control techniques such as DQ-controlled multicarrier SVPWM. This technique enhances power quality by mitigating harmonic distortions and ensuring a stable and high-quality power supply to all connected loads and the grid.

This system configuration is a comprehensive and sophisticated structure that optimizes the generation of electricity from a PV array, seamlessly integrates it with the grid, and manages power distribution to various loads while prioritizing power quality through advanced control strategies. It showcases a holistic approach to renewable energy integration and grid connectivity with a focus on efficiency and reliability.

3. Proposed Method

With a focus on the use of a Photovoltaic (PV) array, the suggested technique offers a thorough and complex approach to regulating and controlling electricity inside a renewable energy system. In order to guarantee that the PV array continuously works at its Maximum Power Point (MPP), the

method first makes use of a state-of-the-art mechanism called Maximum Power Point Tracking (MPPT) control. This MPP denotes the precise operating condition in which the PV array produces the most electrical power that is possibly possible.

A DC-DC boost converter is used to adjust the DC power produced by the PV array to the precise voltage requirements of the system. This part is essential in regulating the voltage to the needed DC link voltage of the system. It guarantees that the PV array's power output is best matched to the needs of the system in terms of operation. The system moves on to the crucial step of turning DC power into superior AC power after the voltage adjustment phase. A DC-to-AC converter, also known as an inverter, is used to carry out this conversion.

The outcome is an excellent AC power output that is precisely timed to the utility grid. The synchronization enables the system to seamlessly interact with the grid, allowing it to both draw power from the grid when the PV array's output falls short and supply excess power back to the grid during periods of surplus energy generation. The system's versatility and adaptability come into play when accommodating an array of loads, which includes linear, non-linear, and Electric Vehicle (EV) loads. These loads are characterized by varying power consumption patterns and behaviors. When combined, these different types of loads can potentially introduce power quality issues.

Specifically, the nonlinear loads have the capability to generate harmonics in the power supply, while the dynamic nature of EV charging can lead to fluctuations in power consumption. To effectively address these power quality challenges and ensure that the system delivers stable and high-quality power, the methodology introduces a sophisticated control technique called DQ-controlled multicarrier SVPWM (Space Vector Pulse Width Modulation). This technique is integral in regulating the AC voltage, eliminating undesirable harmonic distortions, and proficiently balancing loads. Moreover, it involves the precise calculation of reference supply currents, which consist of in-phase and quadrature components.

These calculations are facilitated through the use of Proportional-Integral (PI) controllers, which are responsible for adjusting the amplitude of these components based on the system's specific requirements. In this manner, the system is engineered to provide a highly controlled and regulated power supply, with an unwavering focus on achieving and maintaining exceptional power quality.

3.1. Controller Technique

Bidirectional DC-DC converters are designed to facilitate bidirectional energy flow. This means they can transfer electrical energy from one DC source (e.g., a battery, supercapacitor, or photovoltaic array) to another and can reverse the energy flow when needed. This bidirectional capability is vital in scenarios where energy needs to be efficiently managed and shared between different sources or loads.

Table 1. Specification details

Component	Parameters	Role in the System
PV Array	Vmpp: 54.7 V	Primary power source from sunlight
	Voc: 64.2 V	
	Impp: 5.58 A	
	Isc: 5.96 A	
	Series Panels: 6	
	Parallel Panels: 48	
Grid	Voltage: 440 V	Utility power source
	Frequency: 50 Hz	
Transformer	Ratio: 1:1	Voltage level matching
	Rating: 100 kVA, 50 Hz	
Linear Load	Power: 80 kW	Constant power consumption
Non-Linear Load	Components: Rectifier (L=2 mH, R=50)	Harmonic generation
Boost Converter	Vo out: 700 V	Voltage adjustment for DC
	Vin: 300 V	Link
Inverter	Type: 3-level, SVPWM	DC to AC power conversion
PHEV (EV Load)	Battery: 120 V li-ion (50 Ah)	Electric vehicle charging

Bidirectional DC-DC converters are usually controlled by adjusting the output voltage and current to the needs of the energy storage components or connected devices. Proportional Integral (PI) controllers, among other control algorithms, are frequently employed to maintain the intended voltage and current levels seen in Figure 2.

The reference supply currents' in-phase component (I*spd) magnitude is measured using a Proportional-Integral (PI) controller. This computation is predicated on the system's average DC bus voltage (Vdca) as compared to its reference value.

A voltage error known as a Vdc error is produced when the reference and average DC bus voltage values differ from one another. To calculate the PI controller's output error, the magnitude of the in-phase component (I*spd) in the reference supply currents is utilized.
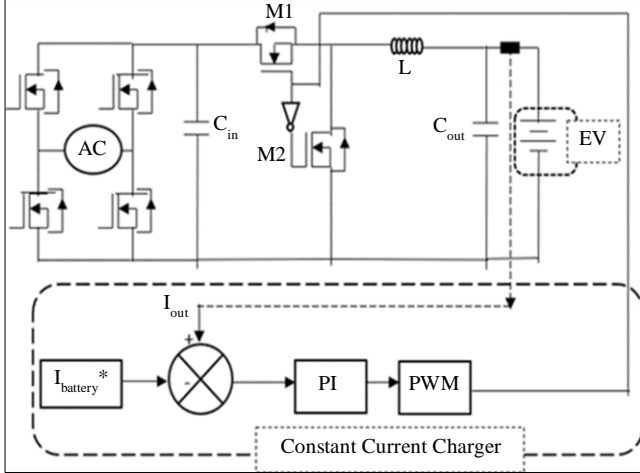
Fig. 2 Bidirectional DC-DC converter controls

The three-phase in-phase components of the reference supply currents can be precisely determined by using this magnitude (I*spd) and the in-phase unit current vectors, which are naturally aligned with the supply voltages.

This method guarantees that the reference supply currents' in-phase components can be precisely controlled and managed by the system. For calculating the magnitude (I*spd) of the quadrature component in the reference supply currents, another Proportional Integral (PI) controller is used. This specific calculation is based on the average supply voltage amplitude (Vspa) relative to the reference value (Vsp*).

A voltage error, known as a Vsp error, is produced when the system compares the average value of the source voltage's amplitude with the reference value. By combining the direct-axis current with the in-phase unit currents, usad, usbd, and uscd, the system creates the three-phase direct current and quadrature current references. By dividing the instantaneous value by the amplitude, these unit currents can have values that vary between 0 and 1.

This method further improves the control and regulation capabilities of the system by guaranteeing the accurate estimation of the in-phase and quadrature components of the reference supply currents. The quadrature component in the reference supply currents and its magnitude (I*spq) are crucial factors to consider when evaluating the output error of the Proportional-Integral (PI) controller.

The three-phase quadrature components of the reference supply currents denoted as I*saq, I*sbq, and I*scq, can be estimated using this number. These components, known as Usaq, Usbq, and Uscq, are obtained from their corresponding amplitude (I*spq) and the quadrature unit current vectors. Interestingly, the in-phase unit current vectors are the source of these unit current vectors. The reference supply currents, which comprise both in-phase and quadrature components, are

utilized directly for several functions, such as controlling the AC voltage, reducing harmonic distortion, and maintaining load balance in the system.

The purpose of purposely setting the amplitude (I*spq) of the quadrature components (I*saq, I*sbq, and I*scq) to zero is to achieve the specific goals of power-factor correction, harmonics reduction, and load balancing. The whole reference supply currents (I*a, I*b, and I*c) in this situation are evolved from the in-phase components (I*sad, I*sbd, and I*scd).

However, the system's flexibility enables the in-phase and quadrature components of the reference supply currents to be given the appropriate amount of weight. By doing so, it becomes feasible to strike a balance that meets the system's specific requirements and is generally acceptable across various operational scenarios. This adaptability ensures that the system can effectively address a range of power quality challenges and maintain the desired level of performance.

$$I^*_{sad} = I^*_{spd} u_{sad}; \quad i^*_{sbd} = I^*_{spd} u_{sbd}; \quad i^*_{scd} = I^*_{spd} u_{scd} \quad (1)$$

Where,

$$u_{sad} = v_{sa} / V_{sp}; \quad u_{sbd} = v_{sb} / V_{sp} \text{ and } u_{scd} = v_{sc} / V_{sp} \quad (2)$$

Where v_{sa}, v_{sb} and v_{sc} are the instantaneous values of the voltages. And the amplitude V_{sp}

$$V_{sp} = \{2/3 (v^2_{sa} + v^2_{sb} + v^2_{sc})\}^{1/2} \quad (3)$$

Similarly, the quadrature axis three-phase reference current is calculated as follows,

$$I^*_{saq} = I^*_{spq} u_{saq}; \quad i^*_{sbq} = I^*_{spq} u_{sbq}; \quad i^*_{scq} = I^*_{spq} u_{scq} \quad (4)$$

Where u_{saq}, u_{sbq} and u_{scq} are calculated by using the following formula,

$$u_{saq} = (- u_{sbd} + u_{scd})\sqrt{3}$$

$$u_{sbq} = (- u_{sad} \sqrt{3} + u_{sbd} - u_{scd}) / (2\sqrt{3})$$

$$u_{scq} = (- u_{sad} \sqrt{3} + u_{sbd} - u_{scd}) / (2\sqrt{3}) \quad (5)$$

The total of both the direct and the quadrature reference current is shown below.

$$i^*_{sa} = i^*_{sad} i^*_{saq}; \quad i^*_{s}{}^b = i^*_{sbd} + i^*_{sbq}; \quad i^*_{sc} = i^*_{scd} + i^*_{scq} \quad (6)$$

The drawbacks of Sinusoidal Pulse Width Modulation (SPWM) are addressed by Space Vector Pulse Width Modulation (SVPWM), a commonly used and effective modulation technique that is especially useful when used in conjunction with a 3-phase inverter, as illustrated in Figure 3.
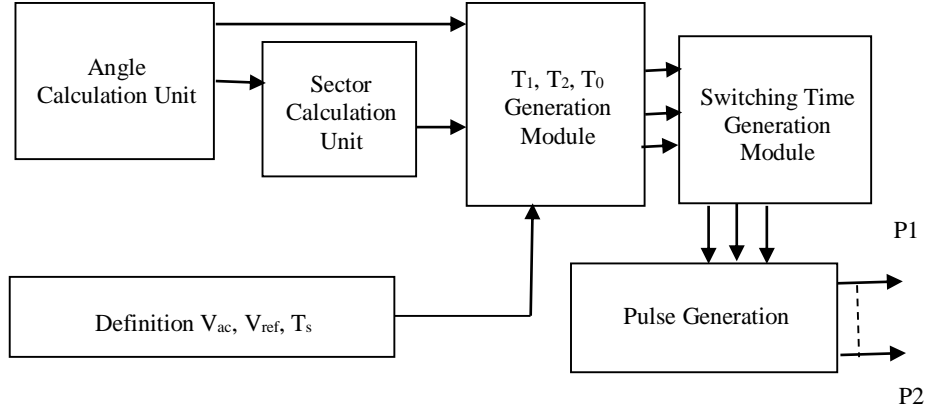
Fig. 3 Space vector pulse width modulations

The primary objective of SVPWM is to achieve several key goals: minimize switching losses, decrease harmonic distortion in the generated output, and effectively utilize the DC bus voltage. Compared to conventional SVPWM methods, the proposed SVPWM model offers the advantage of requiring fewer mathematical operations during implementation. This streamlined approach simplifies the control process, making it more efficient and computationally less demanding.

In the typical operation of a 3-phase, 3-level inverter employing SVPWM, there are eight distinct switching states. These states can be categorized into six active states (numbered 1 to 6) and two zero states (designated as 0 and 7). These switching states determine how the inverter manages the flow of electrical power, controlling the generation of the AC output. By skillfully manipulating these states, SVPWM achieves its objectives, enhancing the quality of the output voltage and minimizing energy losses in the inverter.

4. Simulation Results and Discussion

This simulation involves the application of DQ control in a Photovoltaic (PV) power system with the aim of regulating and managing power. The system is designed to connect with various types of loads, including linear, nonlinear, and Plug-in Hybrid Electric Vehicle (PHEV) loads, in order to replicate real-world scenarios encompassing a wide range of load variations.

The study examines three specific scenarios and compares the results, particularly in terms of Total Harmonic Distortion (THD), with a traditional Icos_ controller. These scenarios are as follows:

Scenario I –EV and non-linear load, Scenario II - Fixed EV and varying load (linear or non-linear), Scenario III- Varying EV and varying load (linear and non-linear). Scenarios II and III are analysed with 6 cases given in Table 2.

The analysis also includes an evaluation of power injection at the Point of Common Coupling (PCC) to assess the power quality of the system. The proposed approach involves subjecting the system to a series of load variations in these three distinct case studies. The loads are categorized into three types: linear load, PHEV load, and non-linear load, with the total load being the sum of these components.

4.1. Scenario I

In the first scenario, represented by Case Study C, there is no linear load, but there is a substantial 80 kW non-linear load and a 4.4 kW PHEV load. This combination results in a total load of 84.4 kW. The scenario is characterized by a dominant non-linear load component, which can introduce harmonics and impact the quality of power in the system.

Load Variations Table 2 as indicated below. The benefits of DQ are highlighted in Figure 4, which shows the power performance at the Point of Common Coupling (PCC). The EV battery pack's bidirectionality is demonstrated in Figure 5. Charging (0 to 0.3 seconds) improves the State of Charge (SOC), while discharging (0.3 to 0.6 seconds) depletes SOC. The current direction, managed by the bidirectional converter, is positive during charging (towards the EV battery) and negative during discharging (towards the grid).

Figures 6 and 7 reveal the DQ controller's THD for voltage and current, showing THD within 5%, except for a 4.97% current THD. In Figures 8 and 9, the DQ controller consistently outperforms I-cosØ, reducing THD. DQ's current and voltage THD values are lower (4.72% for current), with I-cosØ exceeding the 5% limit (6.44% for current).

In summary, DQ control effectively maintains THD within limits, preserving the power factor. It achieves a low 3.66% voltage THD. The comparative analysis underscores the DQ controller's superior performance in voltage control and THD reduction.

Table 2. Load variations for case study

Scenario	Case Study	Linear Load in kW	Non-Linear Load in kW	PHEV Load in kW	Total (kW)
Scenario I	C	0	80	4.4	84.4
Scenario II	C1	0	8.8	6.6	15.4
	C2	8.8	0	6.6	15.4
	C3	50	0	6.6	56.6
	C4	0	50	6.6	56.6
	C5	80	0	6.6	86.6
	C6	0	80	6.6	86.6
Scenario III	C1	14	0	10	24
	C2	0	14	10	24
	C3	4	10	10	24
	C4	30	0	30	60
	C5	0	30	30	60
	C6	0	40	60	100
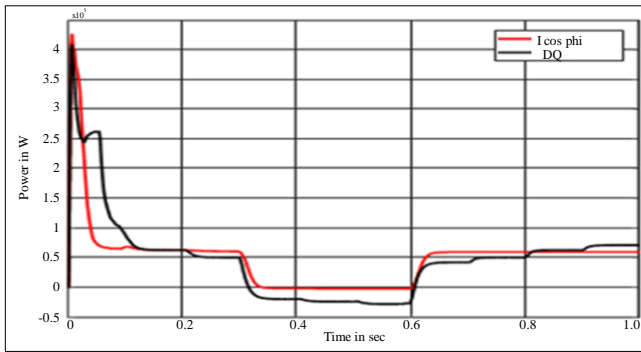
Fig. 4 Power at point of PCC comparison of I-cosØ with DQ control
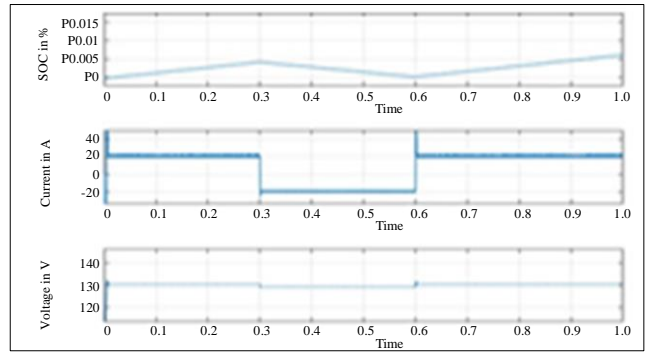
Fig. 5 SOC, current and voltage at EV battery pack
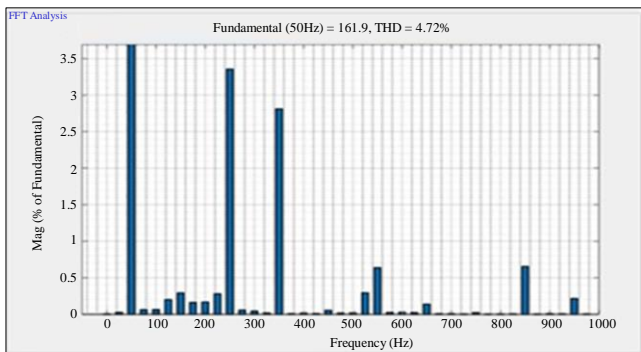
Fig. 6 Current THD for DQ controller
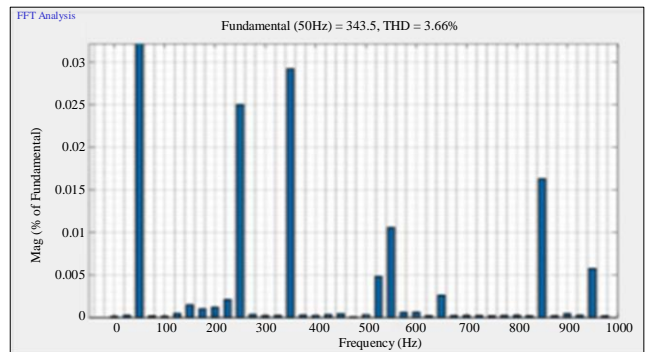
Fig. 7 Voltage THD for DQ controller
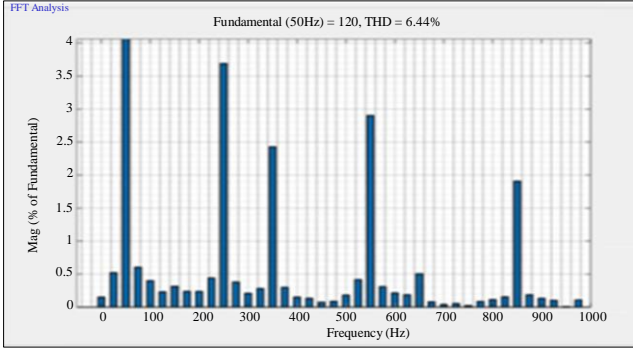
Fig. 8 Current THD for I cos Ø controller
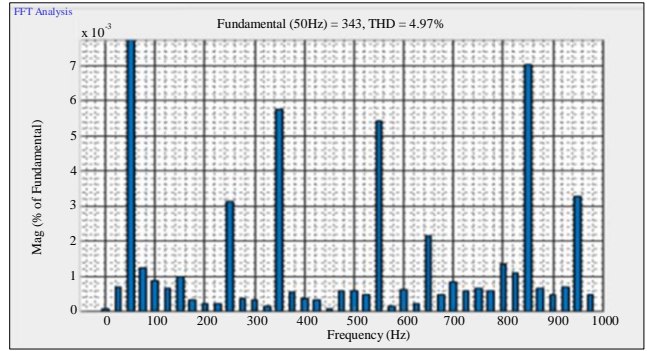
Fig. 9 Voltage THD for I cos Ø controller

4.2. Scenario II

In Scenario II, multiple case studies (C1 to C6) are examined, each featuring different load configurations. C1 exhibits no linear load but has 8.8 kW of non-linear load and 6.6 kW of PHEV load, totalling 15.4 kW. This pattern repeats in the other case studies with variations. Notably, C3 and C4 introduce substantial linear and non-linear loads, respectively, with C5 and C6 showcasing both types of loads. For each of the six load scenarios, Figure 10 shows the power responses in the PV-EV-grid configuration using the DQ controller.

Scenario II situations (a) through (f) all show how to balance power. Figure 11 showcases Scenario II with cases (a) to (f) employing the I-cos Ø controller, and again, all cases exhibit power balancing. The PV system's power production exhibits a stepped pattern as a result of 0.1-second variations in precipitation. Waveforms for load and PCC power reflect how the battery charges and discharges. The PCC directs excess PV power toward the grid, indicating a negative power curve orientation. The values of Voltage and current THD for both DQ and **I cos Ø** controller are tabulated in Table 3.
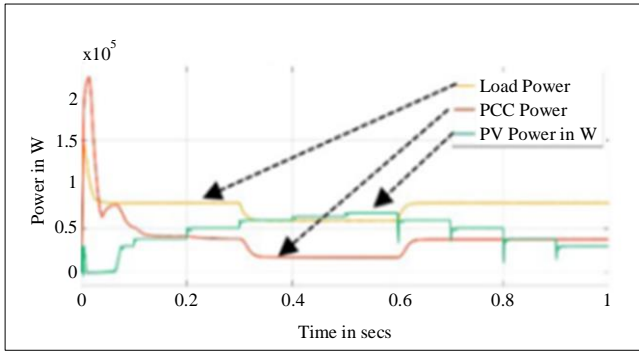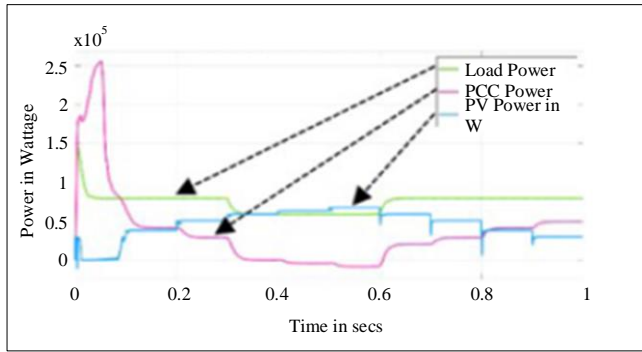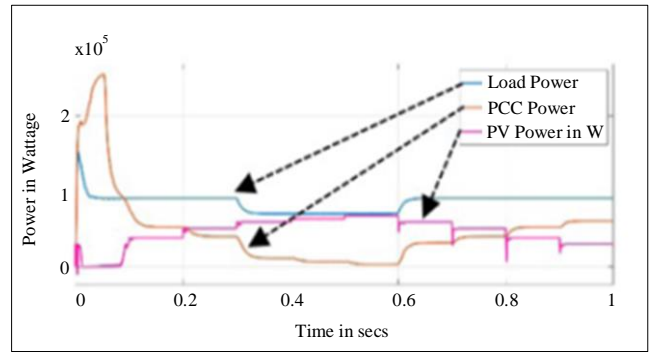

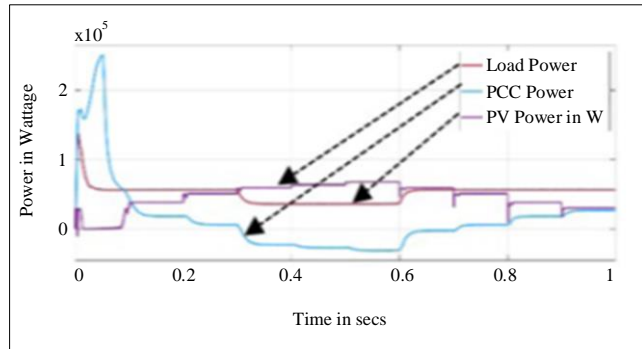**(a)**
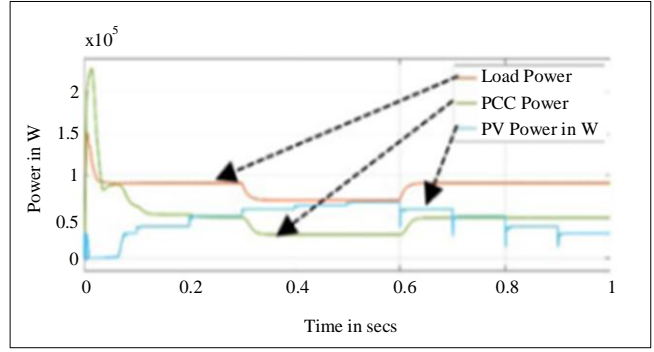
(b)
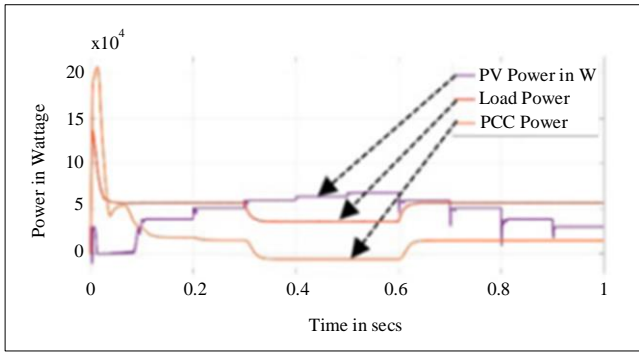
(c)
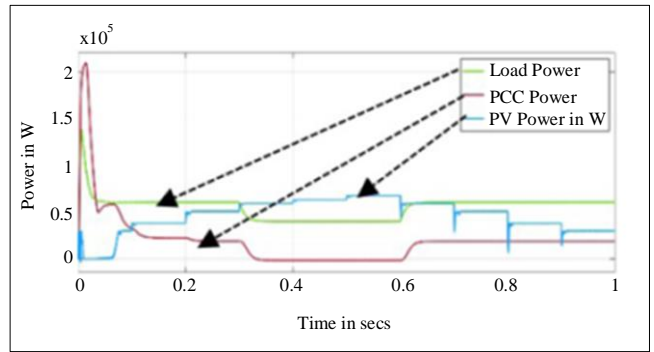
(d)
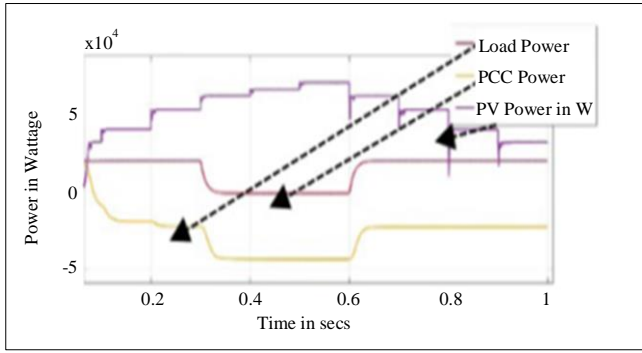
(e)
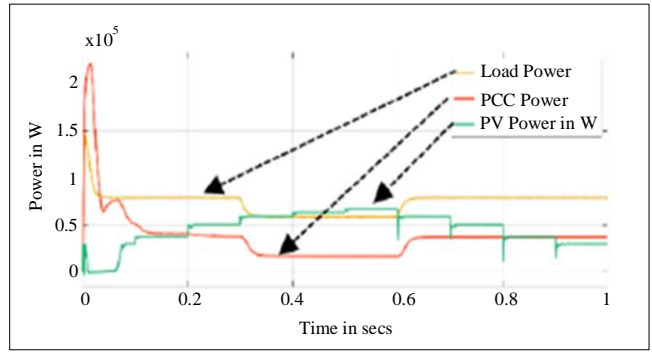
(f)

Fig. 10 Power graph at PCC with DQ controller (scenario II) (a) C1, (b) C2, (c) C3, (d) C4, (e) C5, and (f) C6.
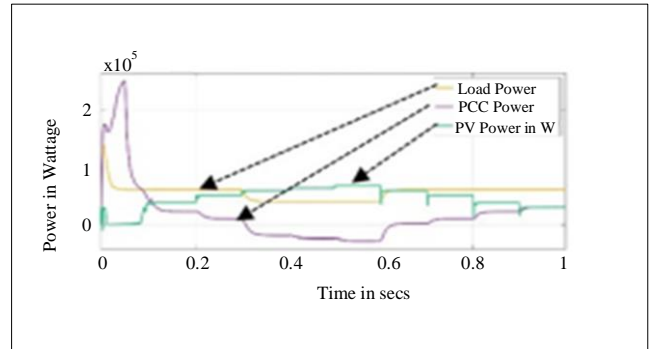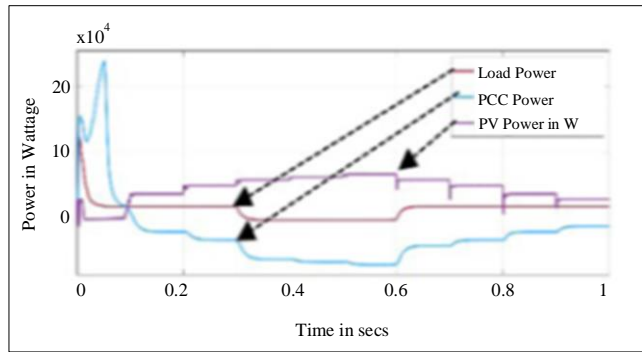

(a)

(b)

(c)

(d)

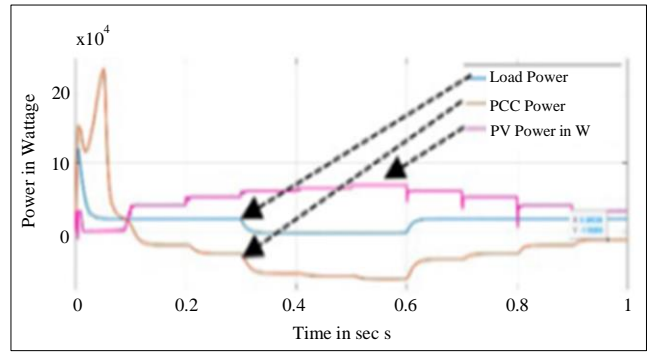**(e)**

(f)

Fig. 11 Power graph at PCC with I cos Ø controller (scenario II) (a) C1, (b) C2, (c) C3, (d) C4, (e) C5, and (f) C6.

Table 3. Voltage and current THD values for DQ and I cos Ø controller

Controller	Case	Voltage THD (%)	Current THD (%)
Scenario I			
DQ Controller	C	3.66	4.72
I cos Ø Controller	C	4.97	`6.44
Scenario II			
DQ Controller	C1	2.6	1.1
	C2	1.9	0.9
	C3	0.6	2.2
	C4	2.3	3.2
	C5	0.4	0.7
	C6	2.3	3.37
I cos Ø Controller	C1	3.4	1.61
	C2	2.9	1.6
	C3	1.2	3.3
	C4	3.3	11.8
	C5	0.8	1.3
	C6	3.3	6.2

Provides a summary of THD, a crucial metric for evaluating grid-connected systems' power quality in each of the three scenarios. The THD study for each of these instances shows that the DQ controller's harmonic mitigation capabilities are superior to that of the other controller.

When comparing the THD percentage using the composite controller (which incorporates the DQ controller) to the I cos Ø approach, a notable improvement in harmonic reduction is noted. This indicates that the composite controller, which includes the DQ controller, performs better in terms of power quality while handling the charging and discharging cycles better than the I cos Ø controller.

4.3. Scenario III
Scenario III mirrors the structure of Scenario II, with a series of case studies (C1 to C6), each presenting diverse load mixtures. For example, C1 incorporates 14 kW of linear load, 10 kW of PHEV load, and no non-linear load, summing up to 24 kW.

Conversely, C2 highlights a nonlinear load, C3 a combination of linear and non-linear loads, and C6 an absence of linear load but a significant non-linear and PHEV load, resulting in a higher total load of 100 kW. The values of Voltage and current THD for both DQ and I cos Ø controller are tabulated in Table 5.

Figure 13 shows the power responses in the PV-EV-grid configuration using the I cos Ø controller. Scenario III situations (a) through (f) all show how to balance power. Figure 14 showcases Scenario III with cases (a) to (f) employing the DQ controller. By examining the maximum power achievements in each load case, we can observe the consistent superiority of the proposed control technique over the conventional method.

Figure 12 demonstrates this in case 1, where the proposed technique achieves a substantial 64.10% improvement, reaching a maximum power of 64 compared to the conventional technique's 39. The trend continues in Figure 12, depicting case 2, with a 66.67% enhancement, as the proposed technique achieves a maximum power of 65 compared to the conventional method's 39.

In Figure 12 (case 3), a substantial 62.50% improvement is evident, with the proposed method reaching 65 units of power, surpassing the conventional approach's 40. Case 4, shown in Figure 12, displays a 65.00% improvement, where the proposed technique achieves a maximum power of 66 compared to the conventional method's 40.

Figure 12 (case 5) exhibits a notable 36.36% enhancement, with the proposed technique achieving 75 units of power while the conventional approach attains 55. Finally, in Figure 12 (case 6), the proposed method excels with a remarkable 75.00% improvement, reaching a maximum power of 100, whereas the conventional method only reaches 25.

In conclusion, by consistently outperforming the conventional method, the proposed technique delivers significant improvements in maximizing power across all cases, as illustrated in the respective figures. Provides data on both the conventional I cos Ø and the proposed DQ techniques, allowing us to compare their respective minimum Total Harmonic Distortion (THD) values across various load cases.
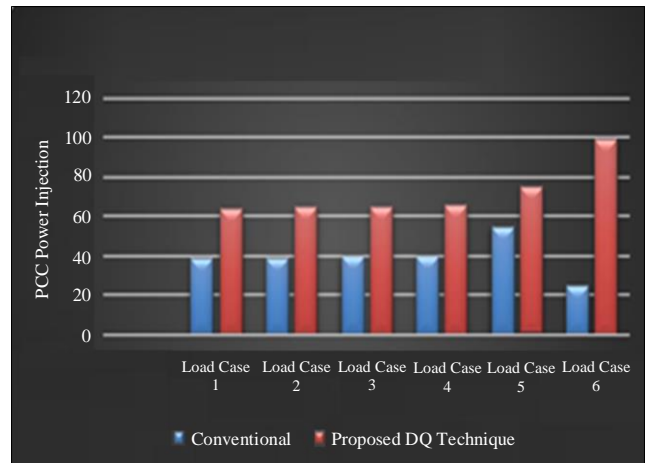
**Fig. 12 PPC power injection comparisons**

The proposed DQ technique consistently delivers lower THD values across all load cases when compared to the conventional **I cos Ø** technique. The improvement percentages range from 36% to an impressive 66%, underscoring the substantial advantages of employing the DQ technique for THD reduction, as tabulated in Table 4.

Table 4. PCC power comparison

Case	Conventional	Proposed DQ Techniques	Improvement in %
Load Case 1	39	64	64
Load Case 2	39	65	66
Load Case 3	40	65	62
Load Case 4	40	66	65
Load Case 5	55	75	36
Load Case 6	25	100	75

Table 5. Voltage and current THD values for DQ and I cos Ø controller

Controller	Case	Voltage THD (%)	Current THD (%)
Scenario III			
DQ Controller	C1	1.37	0.9
	C2	2.27	1.27
	C3	2.03	1.05
	C4	1.33	0.99
	C5	1.33	1.56
	C6	1.33	1.57
I cos Ø Controller	C1	2.53	1.62
	C2	3.32	1.77
	C3	3.14	1.78
	C4	3.55	2.66
	C5	6.59	2.75
	C6	6.19	6.27
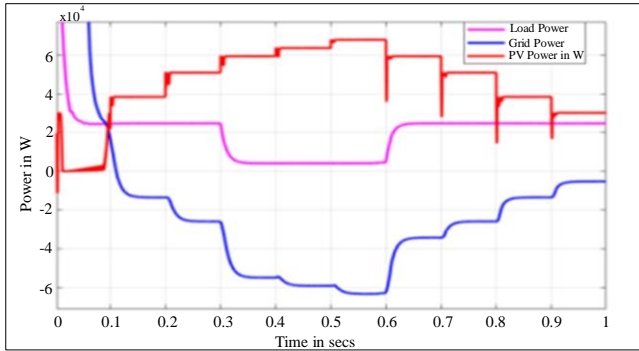
(a)
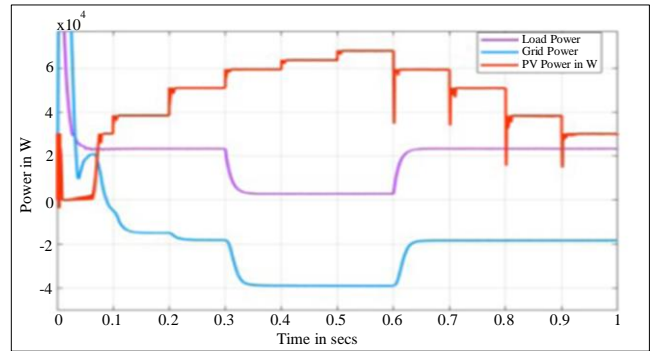
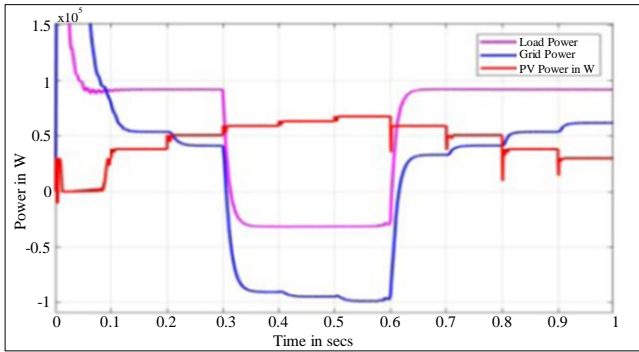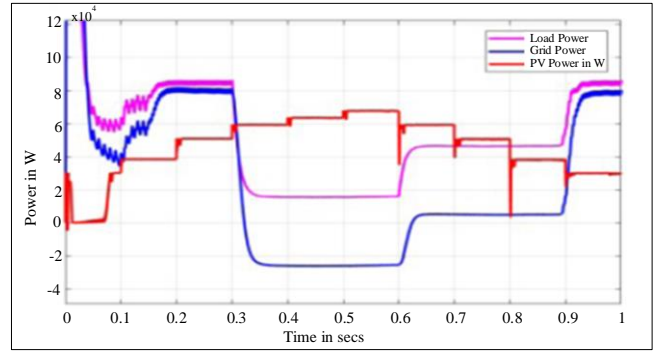

(b)
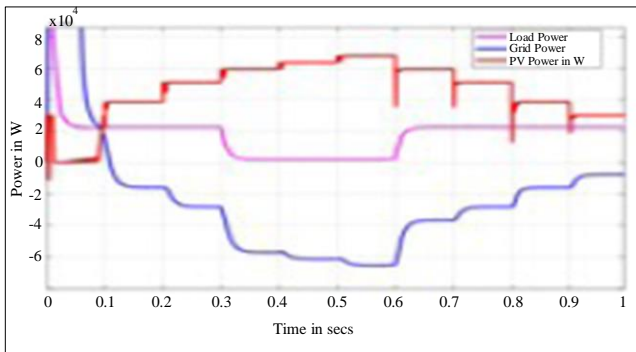
(c)
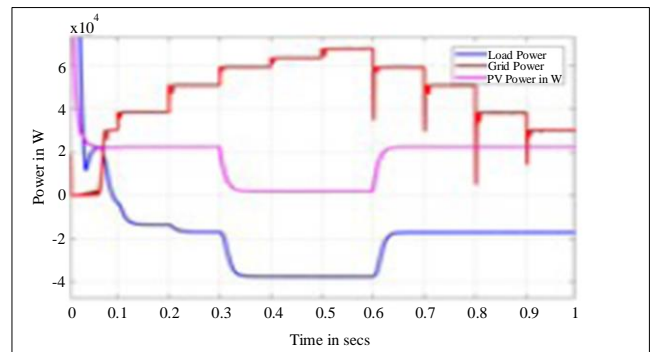
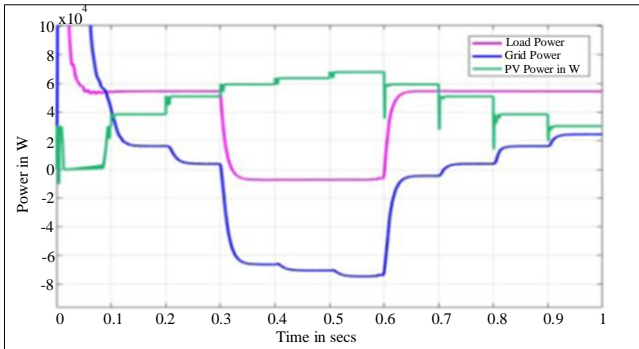**(d)**
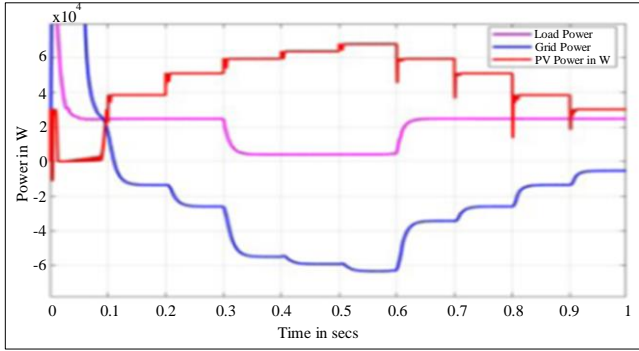
(e)
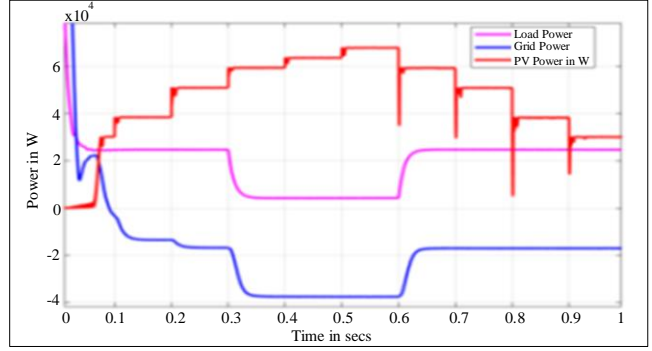
(f)

Fig. 13 Power graph at PCC with I cos Ø controller (scenario III) (a) C1, (b) C2, (c) C3, (d) C4, (e) C5, and (f) C6.
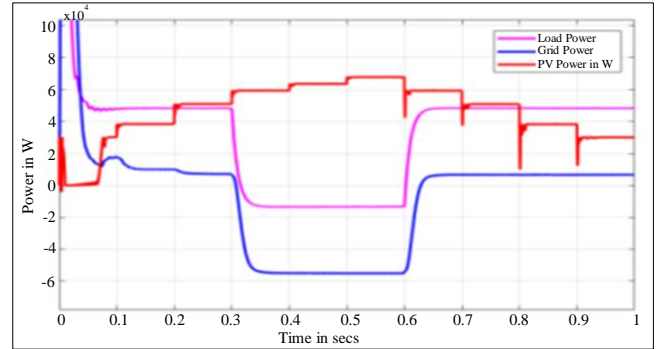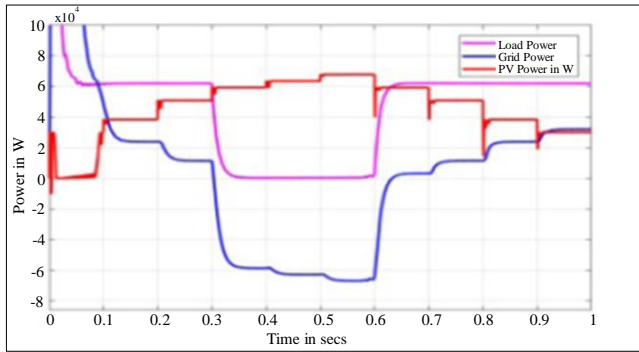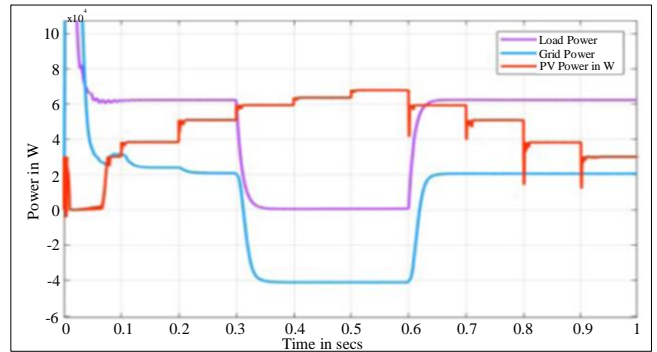

(a)

(b)

(c)

(d)

(e)

(f)

Fig. 14 Power graph at PCC with DQ controller (scenario III) (a) C1, (b) C2, (c) C3, (d) C4, (e) C5, and (f) C6

5. Conclusion

In conclusion, the integration of Photovoltaic (PV) systems and Electric Vehicles (EVs) presents a promising avenue for sustainable energy solutions and reduced environmental impact. The research has demonstrated the effectiveness of advanced control strategies, including the Icos_ controller and dq controller, in regulating voltage, minimizing Total Harmonic Distortion (THD), and enabling bi-directional power flow. Through a comprehensive Simulink model simulating a complex PV-EV-grid system, this study has shown that the THD values meet stringent IEEE 519 standards, emphasizing the success of these integrated control methodologies. The research contributes to the advancement of PV and EV technologies, fostering grid-compatible and high-quality power distribution. This endeavor aligns with the goals of sustainable energy integration and environmental sustainability, making significant progress toward a greener and more energy-efficient future.

The future scope of this research involves refining control strategies for improved PV and EV integration efficiency and scalability. Real-world implementations will be explored, with an emphasis on energy storage solutions and advanced grid interactions. Additionally, economic feasibility and policy considerations will be investigated to accelerate global adoption of PV-EV integration, contributing to cleaner and more sustainable energy practices.

References

[1]   International Energy Agency, Global EV Outlook, 2021. [Online]. Available: https://www.iea.org/reports/global-ev-outlook-2021

[2]   Solar PV Power Capacity in the Net Zero Scenario 2010-2030, 2010. [Online]. Available: https://www.iea.org/data-and-statistics/charts/solar-pv-power-capacity-in-the-net-zero-scenario-2010-2030

[3]   L. Cheng, Y. Chang, and R. Huang, "Corrections to Mitigating Voltage Problem in Distribution System With Distributed Solar Generation Using Electric Vehicles [Oct 15 1475-1484]," *IEEE Transactions on Sustainable Energy*, vol. 7, no. 2, pp. 608-608, 2016. [CrossRef] [Google Scholar] [Publisher Link]

[4]   Anjeet Verma, and Bhim Singh, "Bi-Directional Charger for Electric Vehicle with Four Quadrant Capabilities," *2016 IEEE 7th Power India International Conference (PIICON)*, Bikaner, India, pp. 1-6, 2016. [CrossRef] [Google Scholar] [Publisher Link]

[5]   Justin M. Foster et al., "Plug-In Electric Vehicle and Voltage Support for Distributed Solar: Theory and Application," *IEEE Systems Journal*, vol. 7, no. 4, pp. 881-888, 2013. [CrossRef] [Google Scholar] [Publisher Link]

[6]   Giuseppe Buja, Manuele Bertoluzzo, and Christian Fontana, "Reactive Power Compensation Capabilities of V2G-Enabled Electric Vehicles," *IEEE Transactions on Power Electronics*, vol. 32, no. 12, pp. 9447-9459, 2017. [CrossRef] [Google Scholar] [Publisher Link]

[7]   Morris Brenna, Federica Foiadelli, and Michela Longo, "The Exploitation of Vehicle-to- Grid Function for Power Quality Improvement in a Smart Grid," *IEEE Transactions on Intelligent Transportation Systems*, vol. 15, no. 5, pp. 2169-2177, 2014. [CrossRef] [Google Scholar] [Publisher Link]

[8]   Van-Linh Nguyen et al., "Charging Strategies to Minimize the Energy Cost for An Electric Vehicle Fleet," *IEEE PES Innovative Smart Grid Technologies*, Europe, Istanbul, Turkey, pp. 1-7, 2014. [CrossRef] [Google Scholar] [Publisher Link]

[9]   Pablo Garcia-Trivino et al., "Control and Operation of Power Sources in a Medium-Voltage Directcurrent Microgrid for an Electric Vehicle Fast Charging Station with a Photovoltaic and a Battery Energy Storage System," *Energy*, vol. 115, pp. 38-48, 2016. [CrossRef] [Google Scholar] [Publisher Link]

[10]   Ahmad Hamidi, Luke Weber, and Adel Nasiri, "EV Charging Station Integrating Renewable Energy and Second-Life Battery," *2013 International Conference on Renewable Energy Research and Applications (ICRERA)*, Spain, pp. 1217-1221, 2013. [CrossRef] [Google Scholar] [Publisher Link]

[11]   Longcheng Tan et al., "Comprehensive DC Power Balance Management in High-Power Three-Level DC-DC Converter for Electric Vehicle Fast Charging," *IEEE Transactions on Power Electronics*, vol. 31, no. 1, pp. 89-100, 2016. [CrossRef] [Google Scholar] [Publisher Link]

[12]   Longcheng Tan et al., "Effective Voltage Balance Control for Bipolar-DC-Bus-Fed EV Charging Station with Three- Level DC-DC Fast Charger," *IEEE Transactions on Industrial Electronics*, vol. 63, no. 7, pp. 4031-4041. [CrossRef] [Google Scholar] [Publisher Link]

[13]   Longcheng Tan, Ning Zhu, and Bin Wu, "An Integrated Inductor for Eliminating Circulating Current of Parallel Three-Level DC-DC Converter-Based EV Fast Charger," *IEEE Transactions on Industrial Electronics*, vol. 63, no. 3, pp. 1362-1371, 2016. [CrossRef] [Google Scholar] [Publisher Link]

[14]   Sebastian Rivera, and Bin Wu, "Electric Vehicle Charging Station with an Energy Storage Stage for Split-DC Bus Voltage Balancing," *IEEE Transactions on Power Electronics*, vol. 32, no. 3, pp. 2376-2386, 2017. [CrossRef] [Google Scholar] [Publisher Link]

[15]   Srinivas Bhaskar Karanki et al., "A DSTATCOM Topology with Reduced DC- Link Voltage Rating for Load Compensation with Non-Stiff Source," *IEEE Transactions on Power Electronics*, vol. 27, no. 3, pp. 1201-1211, 2012. [CrossRef] [Google Scholar] [Publisher Link]

[16] Sunil Kumar, and Bhim Singh, "Control of 4-Leg VSC Based DSTATCOM Using Modified Instantaneous Symmetrical Component Theory," *2009 International Conference on Power Systems*, Kharagpur, India, pp. 1-6, 2009. [CrossRef] [Google Scholar] [Publisher Link]

[17] Tejas Zaveri, Bhavesh Bhalja, and Naimish Zaveri, "Comparison of Control Strategies for DSTATCOM in Three- Phase, Four- Wire Distribution System for Power Quality Improvement under Various Source Voltage and Load Conditions," *International Journal of Electrical Power & Energy Systems*, vol. 43, no. 1, pp. 582-594, 2012. [CrossRef] [Google Scholar] [Publisher Link]

[18] Muhammad Ammirrul Atiqi Mohd Zainuri et al., "DC-Link Capacitor Voltage Control for Single-Phase Shunt Active Power Filter with Step Size Error Cancellation in Self- Charging Algorithm," *IET Power Electronics*, vol. 9, no. 2, pp. 323-335, 2016. [CrossRef] [Google Scholar] [Publisher Link]

[19] Sen Ye et al., "Shunt Active Power Filter Based on Proportional Integral and Multi Vector Resonant Controllers for Compensating Nonlinear Loads," *Journal of Electrical and Computer Engineering*, vol. 2018, pp. 1-12, 2018. [CrossRef] [Google Scholar] [Publisher Link]

[20] Tarek A. Kasmieh, and Hassan S. Omran, "Active Power Filter Dimensioning Using a Hysteresis Current Controller," *World Academy of Science, Engineering and Technology*, vol. 52, pp. 233-237, 2009. [Google Scholar]

[21] Mohammad Najjar et al., "Model Predictive Controllers with Capacitor Voltage Balancing for a Single-Phase Five- Level SiC/Si Based ANPC Inverter," *IEEE Open Journal of Power Electronics*, vol. 2, pp. 202-211, 2021. [CrossRef] [Google Scholar] [Publisher Link]

[22] A. Renault et al., "Current Control Based on Space Vector Modulation Applied to Three-Phase H-Bridge STATCOM," *2020 IEEE International Conference on Industrial Technology (ICIT)*, Buenos Aires, Argentina, pp. 1066-1070, 2020. [CrossRef] [Google Scholar] [Publisher Link]

[23] Alfredo Renault et al., "Analysis of H-Bridge STATCOM with Fault Phase Controlled by Modulated Predictive Current Control," *2019 IEEE CHILEAN Conference on Electrical, Electronics Engineering, Information and Communication Technologies (CHILECON)*, Valparaiso, Chile, pp. 1-5, 2019. [CrossRef] [Google Scholar] [Publisher Link]

[24] Alfredo Renault et al., "Modulated Predictive Current Control Technique for a Three-Phase Four-Wire Active Power Filter Based on H-Bridge Two-Level Converter," *2018 53rd International Universities Power Engineering Conference (UPEC)*, Glasgow, UK, pp. 1-6, 2018. [CrossRef] [Google Scholar] [Publisher Link]

[25] Leonardo Comparatore et al., "Finite Control Set Model Predictive Control Strategies for a Three-Phase Sevenlevel Cascade H-Bridge DSTATCOM," *2018 7th International Conference on Renewable Energy Research and Applications (ICRERA)*, Paris, France, pp. 779-784, 2018. [CrossRef] [Google Scholar] [Publisher Link]

[26] Hanying Gao et al., "Seven-Level Active Power Filter Based On A Novel H-Bridge Power Topology Structure," *Eneergies*, vol. 12, no. 15, pp. 1-16, 2019. [CrossRef] [Google Scholar] [Publisher Link]

[27] Yu Wang et al., "A Simplified Minimum DC-Link Voltage Control Strategy for Shunt Active Power Filters," *Energies*, vol. 11, no. 9, pp. 1-14, 2018. [CrossRef] [Google Scholar] [Publisher Link]

[28] Bhim Singh, and Sabha Raj Arya, "Back-Propagation Control Algorithm for Power Quality Improvement Using DSTATCOM," *IEEE Transactions on Industrial Electronics*, vol. 61, no. 3, pp. 1204-1212, 2014. [CrossRef] [Google Scholar] [Publisher Link]